International Journal of Applied Science and Engineering

Effects of upstream and downstream ramp on flow characteristics over a cylindrical weir

Mohammad Akram Saadi AL-Dabbagh[1*], Abdullah Ahmed Shekho[1], Mehmet Ishak Yuce[2], Dheyaa Ghanim Abdulrazzaq[1]

[1] *Northern Technical University, Mosul Technical Institute, Department of Water Resources Techniques, Mosul, Iraq*
[2] *Gaziantep University, Civil Engineering Department, Gaziantep, Turkey*

ABSTRACT

Cylindrical weirs are one of the most commonly employed hydraulic structures to measure flow, compare to other types of the same width they pass larger discharge. This paper presents an experimental work together with a CFD simulation to study the effects of the geometric characteristics of a cylindrical weir and a ramp placed upstream or downstream of the same weir on the discharge coefficient. Three different weir diameters and three ramp angles under three different discharges were utilized. The results show that the geometric characteristics represented by the diameter of the weir affects the discharge coefficient when there is no ramp. The discharge coefficient was observed to decrease as the slope of the upstream ramp was increased, however as the slope of the downstream ramp was increased the discharge coefficient was noted to increase. A mathematical relationship was developed in order to calculate the discharge of flow passes over the cylindrical weir depending on its diameter.

Keywords: Cylindrical weir, Overflow, Upstream ramp, Downstream ramp discharge coefficient, CFD.

Received: August 15, 2022
Revised: January 12, 2023
Accepted: February 13, 2023

Corresponding Author:
Mohammad Akram Saadi AL-Dabbagh
mohamed.akram@ntu.edu.iq

Publisher:
Chaoyang University of Technology
ISSN: 1727-2394 (Print)
ISSN: 1727-7841 (Online)

1. INTRODUCTION

Weirs are barriers across a river designed to change flow of the streams in order to prevent flooding, make waterways operable for inland navigation and measure flow discharge. Although there are many types of weirs, mainly used ones are sharp-crested, circular-crested (cylindrical), broad crested and ogee weirs. The conditions of flow at the weir crest are critical and perform as the upstream regulator of the chute flow. Water flow over weirs and spillways are categorized as rapidly varied flow near the weir crest. Cylindrical weirs have a stable overflow form which lets floating debris to pass with an ease compared to sharp-crested ones. They offer a larger discharge capacity than sharp-crested and broad-crested weirs. Compared to ogee weirs it is simple to design cylindrical weirs (Matthew, 1963; Ramamurthy and VO, 1993; Chanson and Montes, 1997 and 1998; White, 1998).

Applications of cylindrical weirs include inflated flexible membrane dams and roller gates (Anwar, 1967; Chanson, 1996). Cylindrical weirs are classified as short crested weirs; they have the characteristics of both sharp-crested and broad-crested weirs. Streamlines above the crest are curved and have strong acceleration or centrifugal force normal to flow direction. Spillways are the safety structures of dams and projected to accommodate the design flood wave. In order to prevent any probable dam failure, often old dams need to be re-evaluated in terms of the maximum possible flood that their spillways can handle, which may have been altered as a consequence of climate change. Dam failures can pose devastation to life, health, livelihood, belongings and homes of people living in the area. Besides many other benefits, having long term records of rainfall, thus runoff is crucially important.

In order to efficiently convey and distribute water to meet agricultural and industrial requirements, flow measurements and control processes constitute an important aspect of water management. Cylindrical weirs are immersed structures used to measure flow discharge in many hydraulic engineering applications. They also control water level in reservoirs and ponds. Vermoera (1941) has studied the effect of dimensionless components H_1/R, P/R on discharge coefficient C_d. For flow over cylindrical weirs at $H_1/R \leq 1$, Mathew (1963) has developed a simple theory which explains evidently surface tension, viscosity and weir's radius, R, impact on C_d. In addition, Sarginson (1984) has conducted an experimental study, using low weir heights, about the effects of scale on flow characteristics.

This study presents an experimental work together with a CFD simulation in order to study the effects of the geometric characteristics of a cylindrical weir represented by weir radius R and a ramp placed upstream or downstream of the same weir on discharge coefficient, C_d. Three different weir sizes and three different ramp angles were used. A mathematical relationship was developed in order to calculate the discharge of flow passes over the cylindrical weir depending on its diameter.

2. EXPERIMENTAL CHANNEL AND WEIR SPECIFICATIONS

The experiments were conducted in the hydraulic laboratory of the Technical Institute, Mosul, Iraq. The experimental flume has a 20 cm width, 25 cm height and 400 cm length. The channel bed was aluminum while its walls were of glass. Water was supplied into the channel from a cuboid tank by a re-circulating system assembled between the flume, settling basin and the tank. The longitudinal slope of the flume was maintained by a lever jack mounted at the end of the channel. A rectangular weir was used temporary just to measure the flow discharge at the beginning of each run, which was placed at the end of the channel (Fig. 1). In addition, there was a point gauge located on top of the channel to measure the depth of water. Cylindrical weirs used in the experiments were made of plastics and have diameters of 11, 8.1 and 6.3 cm. The weirs were placed perpendicular to the direction of flow at a distance of 2 m from the channel inlet (Fig. 2).

2.1 Experimental Setup and Procedure

The experiments were conducted in order to examine the influence of (i) geometrical characteristics of the weir, (ii) a ramp placed at the upstream of the weir (Fig. 3a), and (iii) a ramp placed at the downstream of the weir (Fig. 3b), on flow past over a cylindrical weir. For the first group of the experiments, three different weir sizes, 11, 8.1 and 6.3 cm were employed. In the second and the third set of the experiments, the diameter of the weir was selected to be 8.1 cm with three different inclination angles of 30° and 45° and 60° with respect to the channel bed.

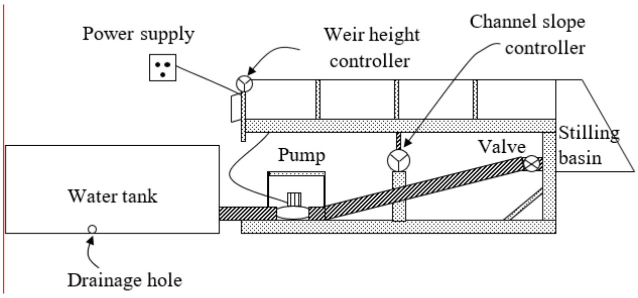

Fig. 1. Experimental channel

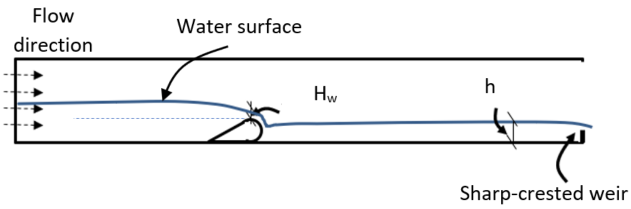

Fig. 2. Experimental measurements

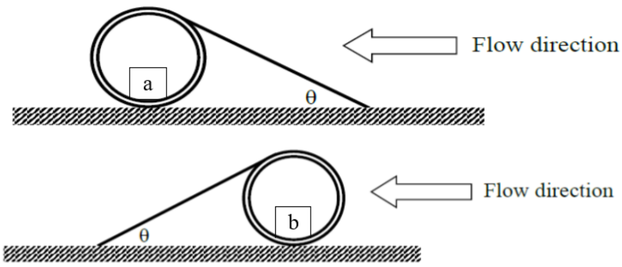

Fig. 3. Side view of models with ramp (a) upstream and (b) downstream

2.2 Dimensional Analysis

In the study of the flow behaviour over cylindrical weirs, the following groups of parameters are relevant (Chow, 1959); (i) Fluid characteristics and physical constants; density of water, ρ_w (kg/m^3), dynamic viscosity, μ_w (N·s/m^2) and acceleration of gravity, g (m/s^2), (ii) Geometry of weir; radius, R (m) or crest height above the channel bed and ramp inclination angle, θ, (iii) Channel Geometry; channel width, b (m), (iv) Upstream flow properties; depth of flow d_1 (m) and flow velocity v (m/s) or the discharge per unit width q_w (m^2/s).

By taking all the above components into account, the dimensional analysis will include the following parameters;

$$F_1\,(\rho_w, \mu_w, g, b, R, d_1, q_w, \theta) = 0 \tag{1}$$

From the components shown above, dimensionless numbers can be determined using π's theorem. In the present study the dimensionless number (H_w/R) and the ramp angle, θ will be dependent in the analysis.

https://doi.org/10.6703/IJASE.202306_20(2).007

2.3 Calculation of Discharge

In order to acquire the discharge, q_w, in the experimental flume, a rectangular non-contractile sharp crested weir of 10 cm height and the Rehbock equation (Humberto, 2009) were employed. The rectangular weir was placed at the end of the channel.

$$q_w = C_d \ x \ \frac{2}{3} \ x \ \sqrt{2g} \ x \ h^{3/2} \tag{2}$$

$$C_{d(weir)} = 0.602 + 0.083 \ x \ \frac{h}{p} \tag{3}$$

Where, P is rectangular sharp crested weir height (in m) and h is water depth at the upstream of the rectangular weir (in m).

2.4 Experimental Results

All the three sets of experiments mentioned above are performed for five different discharge values. Water depth, h, is measured at the upstream of the standard rectangular sharp crested weir in order to calculate the flow rate using Equation 2. In addition, the test section water depth value, H_w, for both the upstream and the downstream ramp, is measured on the top of the cylindrical weir. The measured and simulated flow parameters in Table 1 include the details of the upstream and downstream ramp cases.

The total head, H_1, is calculated by utilizing the following equation (Al-Babely, 2012).

$$H_1 = d_1 + \frac{q_w^2}{2 \ x \ g \ x \ d_1^2} \tag{4}$$

and H_w value is determined by utilizing;

$$H_w = H_1 - D \tag{5}$$

C_d value is estimated by employing;

$$q_w = C_d \ x \ \frac{2}{3} \ x \ \sqrt{\frac{2}{3} \ g} \ x \ H_w^{1.5} \tag{6}$$

Table 1. Measured and calculated parameters for upstream and downstream ramp (D = 8.1 cm)

		Measured		Calculated				
Angle	Run #	h (m)	d_1 (cm)	q_w (m^2/s)	H_1 (m)	H_w (m)	H_w/R	C_d
30° Upstream	1	0.046	12.2	0.0186	0.123	0.042	1.042	1.262
	2	0.04	11.7	0.0150	0.117	0.036	0.910	1.245
	3	0.037	11.5	0.0132	0.115	0.034	0.856	1.208
	4	0.029	10.8	0.0091	0.108	0.027	0.676	1.183
	5	0.031	11	0.0101	0.110	0.029	0.727	1.175
45° Upstream	6	0.045	12.25	0.018	0.123	0.042	1.052	1.202
	7	0.042	11.9	0.016	0.119	0.038	0.962	1.235
	8	0.039	11.7	0.014	0.117	0.036	0.908	1.200
	9	0.034	11.4	0.011	0.114	0.033	0.828	1.114
	10	0.024	10.3	0.006	0.103	0.022	0.549	1.209
60° Upstream	11	0.042	12	0.0161	0.120	0.039	0.986	1.190
	12	0.046	12.3	0.0186	0.124	0.043	1.066	1.220
	13	0.04	11.7	0.0150	0.117	0.036	0.910	1.245
	14	0.038	11.5	0.0138	0.115	0.034	0.858	1.255
	15	0.033	11	0.0111	0.110	0.029	0.729	1.288
30° Downstream	16	0.045	12.4	0.0180	0.125	0.044	1.088	1.142
	17	0.041	12	0.0155	0.120	0.039	0.984	1.149
	18	0.0345	11.3	0.0119	0.113	0.032	0.804	1.191
	19	0.037	11.6	0.0132	0.116	0.035	0.881	1.158
	20	0.028	10.6	0.0086	0.106	0.025	0.626	1.258
45° Downstream	21	0.045	12.2	0.0180	0.1231	0.0421	1.040	1.223
	22	0.04	11.8	0.0150	0.1188	0.0378	0.934	1.196
	23	0.037	11.5	0.0132	0.1156	0.0346	0.856	1.208
	24	0.035	11.15	0.0108	0.1119	0.0309	0.765	1.170
	25	0.024	10.3	0.0068	0.1032	0.0222	0.549	1.209
60° Downstream	26	0.0445	12.15	0.0177	0.122	0.041	1.027	1.225
	27	0.04	11.8	0.0150	0.118	0.037	0.934	1.196
	28	0.036	11.4	0.0127	0.114	0.033	0.831	1.212
	29	0.031	11	0.0101	0.110	0.029	0.727	1.175
	30	0.024	10.4	0.0068	0.104	0.02	0.573	1.132

The correlation between the discharge coefficient, C_d, and the dimensionless parameter H_w/R, was noticed to be a direct proportional relationship for weir diameters of 11 and 8.1 cm (Figs. 4a and 4b). However, an inverse proportional relationship was noted between H_w/R and C_d for weir diameter of 6.3 Fig. 4c. This dispute was explained by Thabet and Mohammed (2010); Vo (1992); AL-Dabbagh et al. (2011) and Yuce et al. (2015), where the curvature of the streamlines represented by increment of flow acceleration. This is explained to be a clear indication that the discharge coefficient of overflow is affected by the geometrical characteristics of the cylindrical weir (Fig. 5).

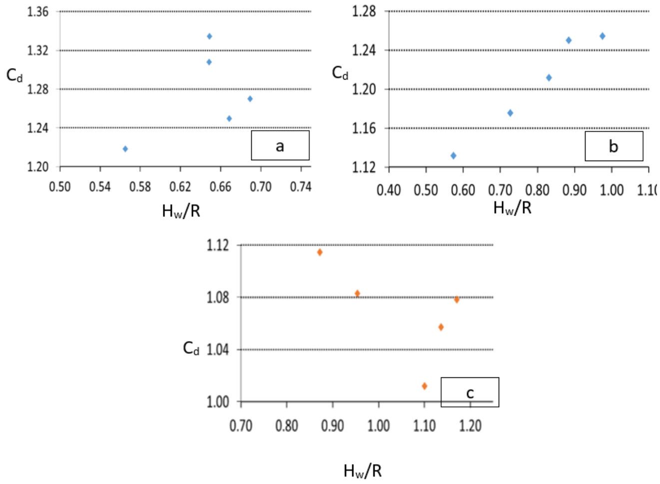

Fig. 4. Relation between discharge coefficients and Hw/R of cylindrical weir (a) D = 11 cm, (b) D = 8.1 cm, (c) D = 6.3 cm

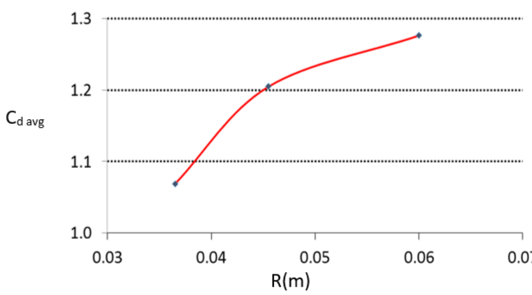

Fig. 5. Proportional relation between average discharge coefficients $C_{d\ avg}$ and radius of model for the first group of experiments

The obtained results are well agreed with the study of AL-Babely (2011), where the discharge coefficient was proportional to the ratio (H_w/R) with a simple deviation due to the existence of ramp in the present study. Moreover, the experimental records are compared with the study of Chanson and Montes (1998), where they used a cylindrical weir with different sizes and situations. In order to validate the present work with the comparative study, a single case is taken, which is the 0.11 m cylindrical weir without ramp, and subjected to a fully- developed flow as taken by Chanson and Montes (1998). The discharge coefficient behaved similarly in the both studies with a shift in the values of (H_w/R) in the comparative study due to the difference only in the channel discharge that results in high values of the variable H_w (Fig. 6).

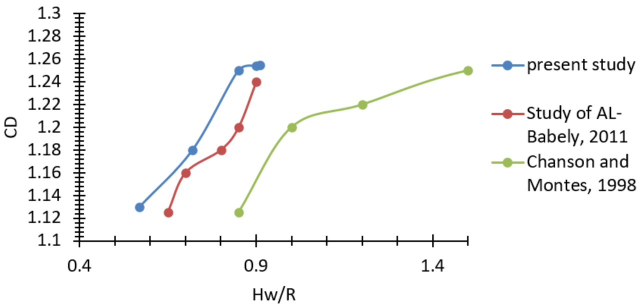

Fig. 6. Comparison of the discharge coefficient behavior against different H_w/Rs' between the present study and the study of AL-Babely (2011) and the study of Chanson and Montes (1998)

Fig. 7 presents the second set of experiments where the ramp was placed at the upstream of the cylindrical weir with inclination angles of 30°, 45° and 60°. The discharge coefficient seems to be slightly affected by H_w/R value when the inclination angle is 30°. This result was also stated by Chanson and Montes (1997). Nevertheless, the discharge coefficient appears to be inversely proportional to H_w/R when the angle of inclination was 60° while at 45° upstream ramp, there is no clear relationship noticed between C_d and the H_w/R.

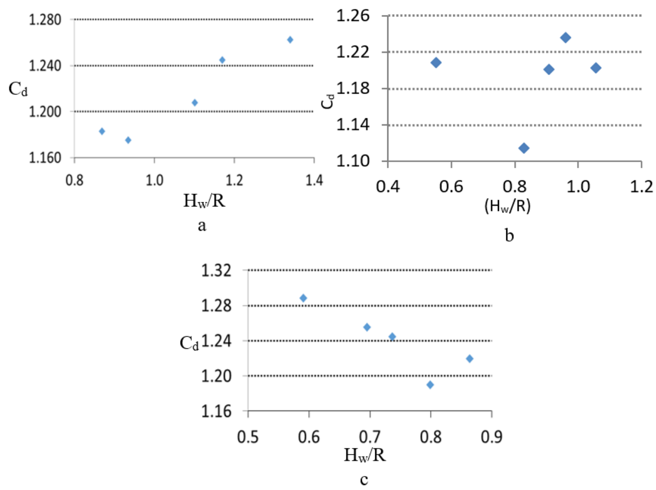

Fig. 7. Relation between discharge coefficients and (H_w/R) of cylindrical weir with upstream ramp. (a) 30°, (b) 45°, (c) 60°

Fig. 8 demonstrates the third group of experiments where a ramp was positioned at the downstream of the cylindrical weir with inclination angles of 30°, 45° and 60°. The discharge coefficient was noticed to be inversely proportional to H_w/R for the inclination angle of 30°. However, for the angle of inclination 60° the discharge coefficient was noticed to be directly proportional to H_w/R. When the angle of inclination is 60° the ramp increases the acceleration of flow at the downstream of the weir contrary to the inclination of 30°, the ramp at the downstream side causes reduction in flow acceleration. Like the 45° upstream ramp, the 45° downstream ramp showed no exact relation between the two variables. Table 2 shows concluded relationships to calculate flow rate depending on the geometry of the model.

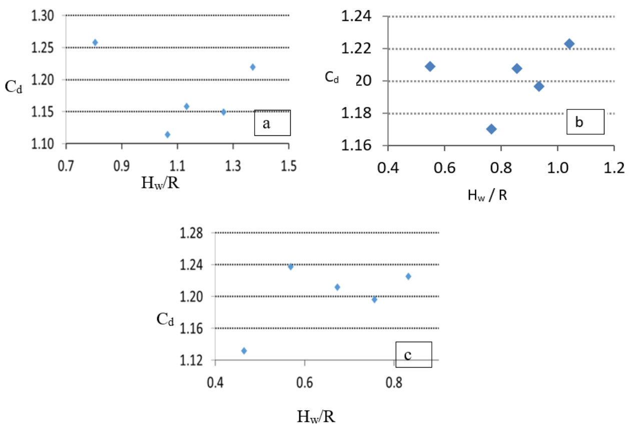

Fig. 8. Relation between discharge coefficients and Hw/R of cylindrical weir with downstream ramp. (a) 30°, (b) 45°, (c) 60°

Table 2. Discharge relationships of model without ramp

	Diameter	Relation	R^2
No ramp	11 cm	$q_w = 92932(d_1)^{8.0983}$	0.93
	8.1 cm	$q_w = 19247(d_1)^{6.5557}$	0.99
	6.3 cm	$q_w = 151.85(d_1)^{4.0617}$	0.97

3. SIMULATION PROCESS

Coefficient of discharge is the ratio of actual flow rate to the theoretical discharge. Therefore, when flow velocity increases, actual discharge increases too, which causes increasing in discharge coefficient value. Simulation analyses are used to study the pattern of the velocity distribution over the weir, which indicates the discharge coefficient's pattern. The numerical investigation includes the cylindrical weir with upstream and downstream ramp. Three inclination angles of (30°, 45° and 60°) were used for the ramp. The diameter of the cylindrical weir model is taken constant as 0.11 m for all cases as in the experimental work. The simulations are conducted under a constant flow situation, which is considered as subcritical flow with a Froude number of 0.5.

3.1 Model Setup

Since decades, many efforts have been made in order to develop simple and efficient numerical models that serve specific and complex flow phenomena. In fluid mechanics, Computational fluid dynamic CFD methods are the most powerful tools used and validated by many researchers in describing and analyzing the fluid-solid interaction in hydraulic installations. In the present study, ANSYS CFX (version 2021 R1) is used to perform number of simulations following the same procedure (including the weir models, the channel and boundary conditions) as in the experiments. An empty channel domain is assumed as an initial condition. A steady-state, which is defined as the case where the flow characteristics do not change with time, multiphase case is dependent in all simulations in order to investigate the interference between air and water flowing in the channel. The two fluids are considered clean with no any suspended loads at a temperature of 25°C. In modeling of open channel flow by ANSYS CFX program, the interface between water and air in an open channel flow is typically modeled using the Volume of Fluid (VOF) method. The VOF method is a multi-fluid modeling technique that tracks the movement and evolution of the interface between two or more fluids. The VOF method represents the interface as a scalar field, which is defined as the fraction of the volume of cells occupied by one of the fluids (e.g. water or air). The value of the VOF field ranges from 0 (fully occupied by the other fluid) to 1 (fully occupied by the current fluid). This allows the VOF method to accurately track the position and movement of the interface between the fluids. In the present study, the boundary conditions and fluid domain are shown in Fig. 9 where the channel left side is considered as an inlet and the right side is an outlet. The top of the domain is performed as an opening assuming that the air is entertaining inside the channel. Other faces of the channel domain with the weir are considered as smooth walls.

3.2 Meshing

The fundamentals of the numerical analyses in most of the simulation programs use the idea of dividing the domain into elements. This process is called meshing. The concept of this procedure is to use the outputs of one element and consider it as an inlet for the next one, and so until reach the solution convergence. It is necessary to mention that the more the elements, the more accurate the results. Hence, save time to reach the convergence.

Each problem has specific meshing procedures, where some regions in a single domain could need to be of a very fine mesh rather than others in order to get further details. Ansys program is provided with different techniques in meshing process to serve many kinds of engineering problems. In the present study, face sizing tool is used on the weir surface to get finer mesh above it. Moreover, a tetrahedron method is used with patch conforming algorithm in order to increase the quality of mesh. Regarding the weir models used in the present study, they are not differing too much from each other. Therefore, similar meshing procedures are followed for all models (Fig. 10).

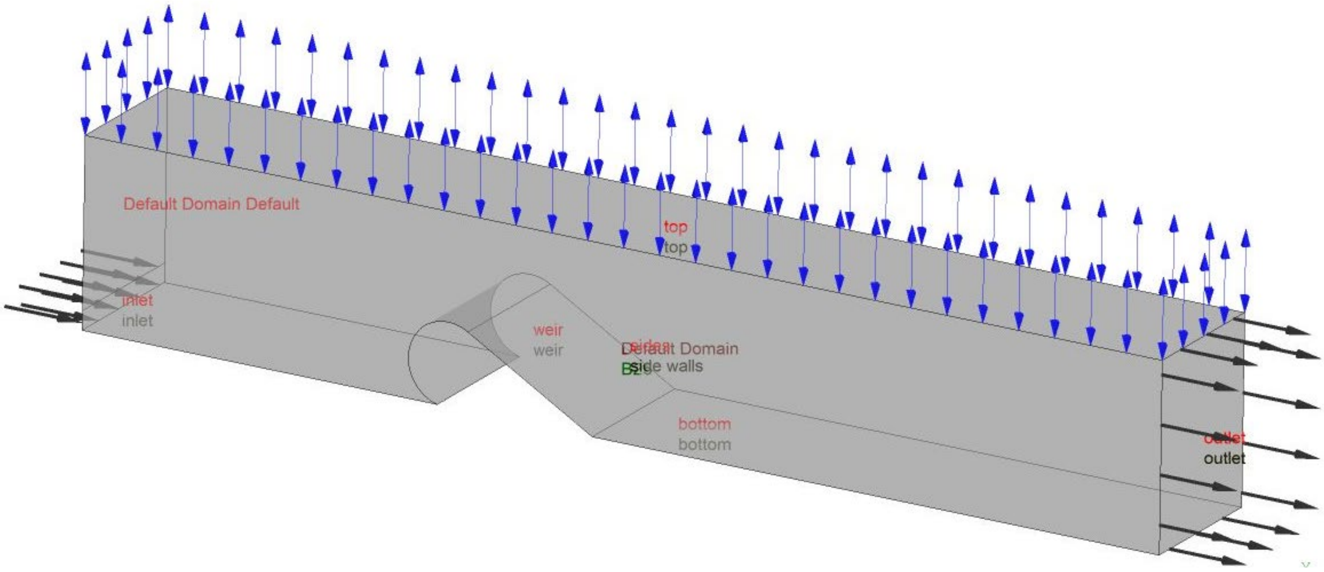

Fig. 9. Boundary conditions and channel domain

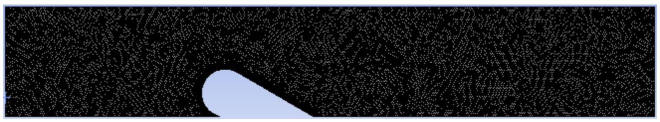

(a)

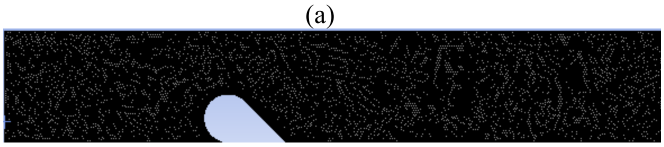

(b)

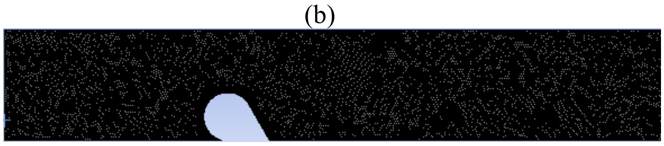

(c)

Fig. 10. Meshing process; (a) 30° ramp, (b) 45° ramp, (c) 60° ramp

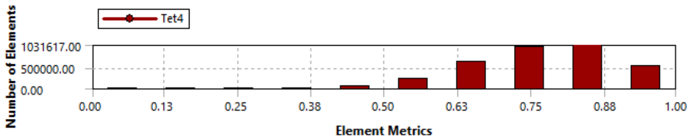

30° Ramp

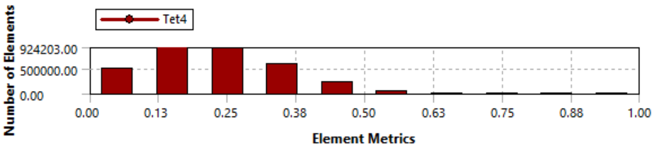

45° Ramp

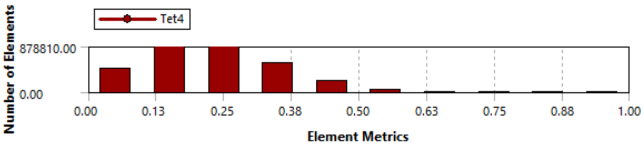

60° Ramp

Fig. 11. Skewness quality test for the three given inclination angles

In order to evaluate the quality of the element meshing, the program uses different testing methods such as the skewness, orthogonal quality, aspect ratio, etc. The skewness test is a measure used to assess the quality of mesh for the weir models under study. This test is used to check whether the elements in the mesh are distorted or skewed, which can affect on the accuracy and convergence of the solution progress. The skewness test checks the angle between the element edges and the element faces to determine whether the element is skewed. If the skewness of an element is too high, it can cause problems with the simulation, such as poor convergence or inaccurate results. The obtained results from meshing process shows that the average skewness value is about 0.22, in average, for all models, which is considered according to meshing standards as an excellent cell quality, Fig. 11.

3.3 The Turbulent Model

In fluid dynamics, the crucial issue that take focus of many researchers is how to describe precisely different flow phenomena that are expected to be occurred around hydraulic structures. Several numerical models were developed to serve different cases. The k-ε turbulent model, which describes the kinetic energy of the fluid and the related energy dissipation, is commonly used in fluid dynamic problems where complex flow regions or large eddies are not expected to be occurred. Later, this model is developed to include the boundary layer effect. For large eddies regions, the large eddy simulation turbulent model LES could be much more efficient than others. In the present work, no complex flow is expected to be created due to the obstruction, therefore, the k-ε turbulent model is dependent in the simulation part, where the channel flow is considered as turbulent flow. This model uses two governing equations related to kinetic energy and energy dissipation. The kinetic energy part of this model is represented by the following equation:

$$\frac{\partial(\rho k)}{\partial t}+\frac{\partial(\rho k u_i)}{\partial x_i}=\frac{\partial}{\partial x_i}\left[\frac{\mu_t}{\rho_k}\frac{\partial k}{\partial x_i}\right]+2\mu_t E_{ij}E_{ij}-\rho\epsilon \quad (7)$$

The second part of k-ε model is the energy dissipation, which is described by the following equation:

$$\frac{\partial(\rho \epsilon)}{\partial t}+\frac{\partial(\rho \epsilon u_i)}{\partial x_i}=\frac{\partial}{\partial x_i}\left[\frac{\mu_t}{\rho_\epsilon}\frac{\partial \epsilon}{\partial x_i}\right]+C_{1\epsilon}\frac{\epsilon}{k}2\mu_t E_{ij}E_{ij}-C_{2\epsilon}\rho\frac{\epsilon^2}{k} \quad (8)$$

Where u_i is the velocity component in the flow direction; E_{ij} is the deformation rate; μ_t is the eddy viscosity; $C_{1\varepsilon}$ and $C_{1\varepsilon}$ are adjustable constants equal to 1.44 and 1.92, respectively.

3.4 Numerical Validation

Since decades, the computational fluid dynamics (CFD) methods proved the ability of describing the flow behavior and the related phenomena numerically. However, all the numerical models should be validated before use. In the present study, the turbulent model, which is k-ε model, is validated against the numerical study of Shahjahan et al. (2017). In one of the comparative studied cases, they used the k-ε turbulent model in order to simulate the flow around a single groin of 90° orientation angle at a constant discharge of 0.043 m^3/s. Similar flow condition was taken for the validation of the numerical model. The channel slope is taken as 0.001 and the bed roughness 0.01 as in the comparative study. The velocity distribution along the channel domain was dependent as a measure of the model accuracy. Fig. 12 shows good agreement with study of Shahjahan et al. (2017) in the velocity distribution represented by velocity contour lines, where the wake region is created behind the groin, which decelerated the flow velocity at that region. Nevertheless, the flow velocity over the groin increased much more than the upstream flow velocity. These findings were well agreed with the comparative study, which proved the adequacy and accuracy of the turbulent model and revealed that it is possible to use the k-ε turbulent model in analyzing the flow behavior around hydraulic installations.

3.5 Simulation Results

The simulation work performed in this study includes investigation the effect of smooth ramp existence upstream or downstream a cylindrical weir. Three different inclination angles of ramp are taken, 30°, 45°, 60°. In order to compare between the results, a single flow condition is dependent, which is subcritical flow at a Froude number of 0.5. The turbulent model, which is k-ε model, will be dependent for all simulation analyses.

It is obvious from Fig. 13 that the velocity values in the case of 30° inclination is larger than those of 45° and 60° inclinations when the ramp was positioned at the upstream of the weir. This is because of velocity break due to 60° inclined upstream ramp, while at 30° inclination angle, the upstream water is flowing smoothly.

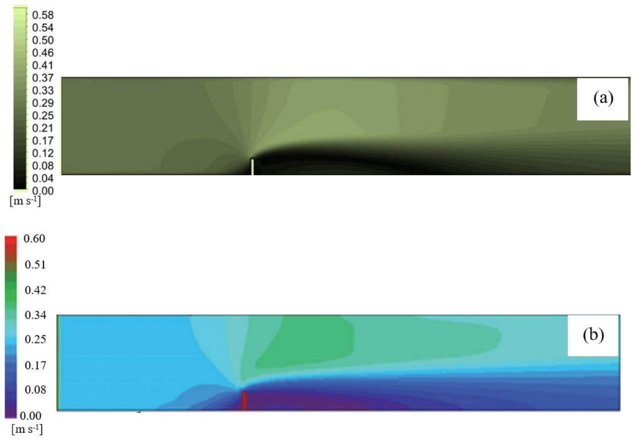

Fig. 12. Velocity contour lines for numerical model validation: (a) the present study, (b) the study of Shahjahan et al. (2017)

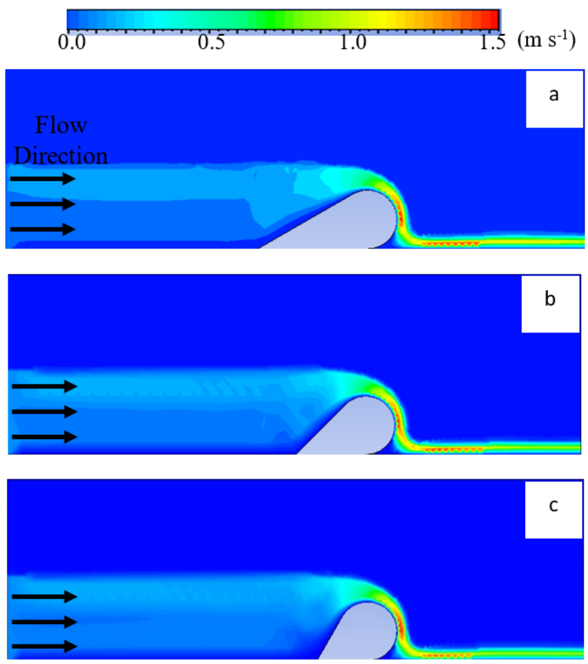

Fig. 13. Velocity distribution of (D = 11 cm) with upstream ramp: (a) 30°, (b) 45°, (c) 60°

The results obtained from the simulation processes have also showed that the downstream ramp is significantly affecting on the velocity distribution. The 60° ramp located at downstream of the weir increases the accelerating force besides curvature of the weir crest. As a result, velocity values increase too. While at 30° inclination of the ramp placed at the downstream of the weir, stream flow becomes smooth because of the long face of the ramp that calms the flow as shown in Fig. 14.

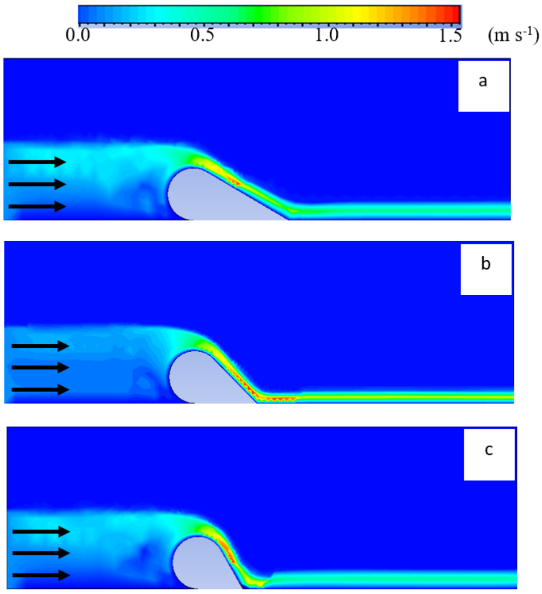

Fig. 14. Velocity distribution of (D = 11 cm) with downstream ramp: (a) 30°, (b) 45°, (c) 60°

In addition, the simulation process is used to study the pressure distribution over the weir (Figs. 15, 16). Regarding the 30° inclination angle, the case of upstream ramp, the flow velocity over the weir crest was high and resulted in low pressure. However, the downstream case shows an inverse behavior due to the existence of the ramp that decelerates the falling water from the weir crest due to less curvature at the downstream face of the structure. The total pressure over the weir, in case of upstream ramp, increases gradually as the inclination angle increases too. This is attributed to the existence of ramp at the upstream face, which breaks down the flow velocity and hence increases the pressure. Nevertheless, the pressure in the case of downstream ramp decreases as the inclination angle increases due to the curvature interruption at the downstream face because of the tangent ramp to the weir (Table 3).

It is valuable to mention that it is important to do 3D simulation analyses, if available, in order to see if the water level over the weir is constant along the weir crest or not. Moreover, the location of hydraulic jump, if any, will be clearer than 2D analyses. The velocity distribution is sketched on water surface profile for all cases to observe flow patterns in case of ramp positioned at the upstream or downstream of the 1 cylindrical weir, Fig. 17. Moreover, a single case is used as a measure of the correlation between the experimental records and simulation measurements, which is the case of the 30° downstream ramp combined with the 11 cm cylindrical weir. Water surface profile is used as a measure of the agreement between them. Fig. 18 shows good agreement with a slight change in the water level at the inlet due to instability of the water entering into the experimental channel unlike the numerical model where this issue could simply be controlled by the program.

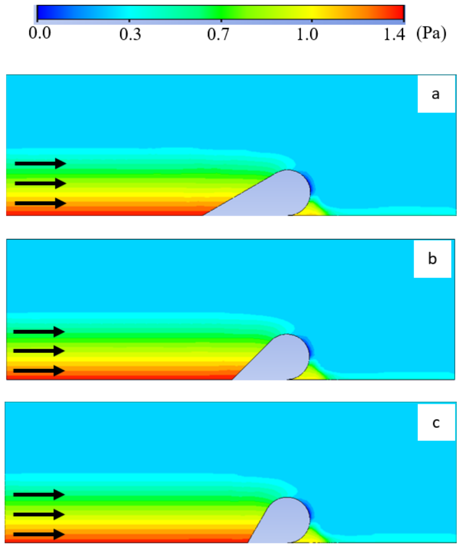

Fig. 15. Pressure distribution of (D = 11 cm) with upstream ramp: (a) 30°, (b) 45°, (c) 60°

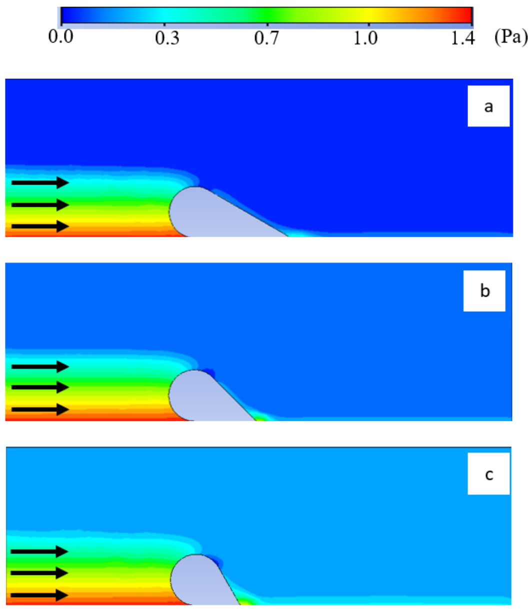

Fig. 16. Pressure distribution of (D = 11 cm) with downstream ramp: (a) 30°, (b) 45°, (c) 60°

Table 3. Maximum pressure over the weir for all the given cases (Pa)

Inclination angle	Upstream ramp	Downstream ramp
30°	413.59	500.26
45°	457.82	448.56
60°	469.21	413.82

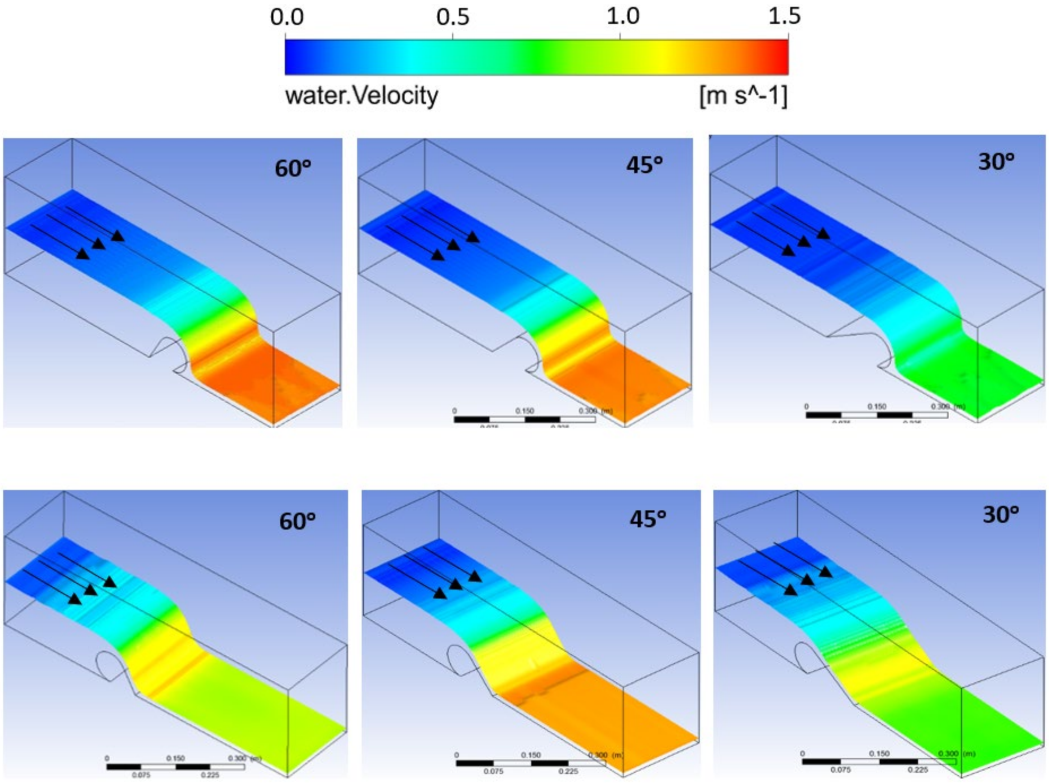

Fig. 17. Velocity distribution in the whole domain at different inclination angles of ramp

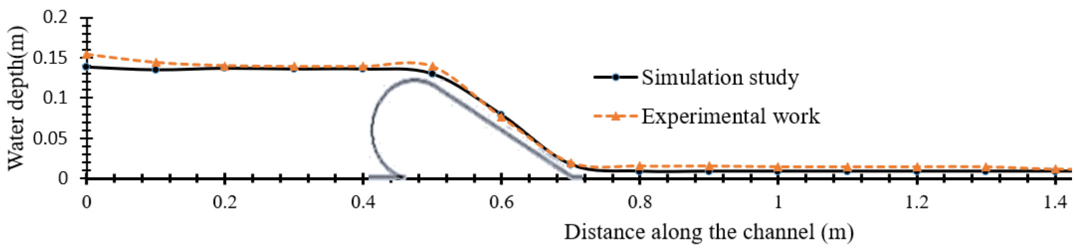

Fig. 18. Experimental and simulated water surface profiles at 30° downstream ramp

4. RESULTS AND DISCUSSIONS

In fluid dynamics, any hydraulic installation could disturb the streamlines. As a result, the flow behavior becomes unstable and different with the distance along the channel length and returns to what it was in the beginning after a certain distance. In the present work, the simulation results show that the upstream or downstream ramp has significant effect on the flow over weirs. The length and angle of the ramp play an important role in the performance of the hydraulic obstacles. These results were well agreed with the study of Manafpour and Ebrahimnezhadian (2019) where they used CFD methods in order to simulate the air flow around a ramp in a pressurized tunnel and their results showed that inclination angle of ramp was the most influential element that affects the flow more than the ramp height. This study contributes to a variety of engineering fields such as cars designs and some hydrokinetic turbines. In addition, CFD techniques have proven their efficiency in simulating the flow and representing it very close to reality (Memon et al., 2012; Yuanyuan et al., 2012; Schleicher et al., 2013; Manafpour and Ebrahimnezhadian, 2019; Tokyay and Kurt, 2019; Lopez Mejia et al., 2021).

5. CONCLUSIONS

This paper presents an experimental work together with a CFD simulation in order to study the effects of the geometric characteristics of a cylindrical weir and a ramp placed upstream or downstream of the same weir on the discharge coefficient. Three different weir diameter sizes were used for the weir and two angles for the ramp. The results show that the geometric characteristics represented by the radius of the weir affects the discharge coefficient when there is no ramp. When the diameter of the model is D ≥ 8 cm the centrifugal force (normal to the flow direction) will increase, as a result, the discharge coefficient will increase too.

When the ramp was placed at the upstream of the weir, it was noticed that with increasing ramp slope angle, discharge coefficient decreases. In case of 30° inclination of ramp situated at upstream of the weir, discharge coefficient was slightly affected by H_w/R value; while the inclination angle was 60° the discharge coefficient was found to be inversely proportional to H_w/R. This is because of the fact that the ramp placed at the upstream of the weir with an inclination angle of 60° acts as a significant obstacle in the waterway, causing low discharge coefficient.

While the ramp was placed at the downstream of the weir, it was observed that increasing the ramp slope angle causes increasing in the discharge coefficient. When the ramp was placed at an angle of 30° at the downstream of the weir, the discharge coefficient was observed to be inversely proportional to H_w/R. This causes reduction in flow velocity, thus the value of C_d. While the inclination angle was 60° the discharge coefficient was noted to be directly proportional to H_w/R, in this case the ramp causes increment in the flow acceleration, therefore increase in the discharge coefficient.

REFERENCES

Al-Babely, E.A. 2012. Behavior of the discharge coefficient for the overflow characteristics of oblique circular weirs. Tikrit Journal of Engineering Sciences, 19, 55–64.

AL-Dabbagh, M.A., AL-Zubaidy, S.D. 2018. Evaluation of flow behavior over broad-crested weirs of a triangular cross-section using CFD techniques. The Eurasia Proceedings of Science, Engineering & Mathematics (EPSTEM), 361–367.

AL-Dabbagh, M.A., Al-Babely, E.A., AAl-Muhammad, A.A. 2011. Overflow characteristic of cylindrical shape crest weirs over horizontal bed. Tikrit Journal of Engineering Sciences, 18, 29–39.

Ali, M., Hasan, M., Haque, M. 2017. Two-dimensional simulation of flows in an open channel with groin-like structures by iRIC Nays2DH. Mathematical Problems in Engineering, 2017.

Anwar, H.O. 1967. Inflatable dams. Journal of the Hydraulics Division, 93, 99–119.

Chanson, H., Montes, J. 1998. Overflow characteristics of cylindrical weirs: Effects of inflow conditions. Journal of Irrigation & Drainage Engineering, ASCE, 124, 152–162.

Chanson, H., Montes, J.S. 1997. Overflow characteristics of cylindrical weirs.

Chanson, H. 1996. Some hydraulic aspects during overflow above inflatable flexible membrane dam (No. CH47/86). Department of Civil Engineering, University of Queensland.

Chow, V.T. 1959. Open channel hydraulics. McGraw-Hill Book Co. Ltd., London.

Humberto, A. 2009. Flow over a Sharp Crested weir. PhD. Thesis, University of Alabama, Department of Civil, Construction and Environmental Engineering, USA.

Lopez Mejia, O.D., Mejia, O.E., Escorcia, K.M., Suarez, F., Laín, S. 2021. Comparison of sliding and overset mesh techniques in the simulation of a vertical axis turbine for hydrokinetic applications. Processes, 9, 1933.

Manafpour, M., Ebrahimnezhadian, H. 2019. Investigating the effect of ramp geometry on the flow characteristics around under pressure tunnel aerator using openfoam open source software. Engineering, Technology & Applied Science Research, 9, 3705–3710.

Mathew, G.D. 1963. On the influence of curvature, surface tension and viscosity on flow over round-crested weirs. Proceedings of the Institution of Civil Engineers, London, 25, 511–524.

Memon, A.A., ABBASI, H.U., ABBASI, A.F., ASAD, M. 2012. Modelling and simulation of flow around wind turbine blade by using actuator surface model. The Sindh University Research Journal (Science Series), 44, 695–698.

Montes, J.S. 1964. On the influence of curvature, surface tension and viscosity on flow over round-crested weirs. Discussion. Proceedings of the Institution of Civil Engineers, London, 28, 562–563.

Ramamurthy, A.S., VO, N.D. 1993. Characteristics of circular-crested weir. Journal of Hydraulic Engineering, ASCE, 119, 1055–1062.

Sarginson, E.J. 1984. Scale effects in model tests on weir. In Symposium on Scale Effects in Modelling Hydraulic Structures, Esslingen, Germany, 3, 1–4.

Schleicher, W.C., Riglin, J.D., Kraybi, Z.A., Oztekin, A. 2013. Design and simulation of a micro hydrokinetic turbine. Proceedings of the 1st Marine Energy Technology Symposium METS13, Washington, D.C.

Thabet, M.A., Mohammed, S.A. 2010. Calibrating the Discharge Coefficient of Semicircular Crested Weir. Engineering and Technology Journal, 28.

Tokyay, T., Kurt, C. 2019. Application of VOF and k-ε turbulence model in simulation of flow over a bottom aerated ramp and step structure. Water SA, 45, 278–290.

Verwoerd, A.L. 1941. Calcul du debit de deversoirsdenoyes et noyes a cretearrondie. L'Ingenieur des IndesNeerlandaises. (translated), 8, 65–78.

Vo, N.D. 1992. Characteristics of Curvilinear Flow Past Circular-Crested Weirs. PhD. Thesis, Civil Engineering, Concordia University, Canada.

White, Frank, 1998. Fluid Mechanics. University of Rhode Island, WCB McGraw-Hill, Fourth Edition.

Yuanyuan X., Jingqi, Y., Jens-Uwe, R., Guenter, W. 2012. CFD study on liquid flow behavior on inclined flat plate focusing on effect of flow rate. Engineering Applications of Computational Fluid Mechanics, 6, 186–194.

Yuce, M.I., Al-Babely, A.A.H., Al-Dabbagh, M.A. 2015. Flow simulation over oblique cylindrical weirs. Canadian Journal of Civil Engineering, 42, 389–407.